Pedestrian Behavior at Signalized Crosswalks in Rainy Conditions: Calibration and Simulation

Hua-yu DENG [a], William H.K. LAM [b], Mei Lam TAM [c], Peng ZHANG [d], Agachai SUMALEE [e]

[a,d] *Shanghai Institute of Applied Mathematics and Mechanics, Shanghai University, Shanghai 200072, PR China*
[a,b,c,e] *Department of Civil and Environmental Engineering, The Hong Kong Polytechnic University, Hung Hom, Kowloon, Hong Kong*
[a] *School of Mathematics and Physics, Shanghai University of Electric Power, Shanghai 200090, PR China*
[a] *E-mail: hydeng@shiep.edu.cn*
[b] *E-mail: william.lam@polyu.edu.hk*
[c] *E-mail: trptam@polyu.edu.hk*
[d] *E-mail: pzhang@mail.shu.edu.cn*
[e] *E-mail: ceasumal@polyu.edu.hk*

Abstract: Walking behavior at signalized crosswalks or passageways in rainy conditions can differ from that in other conditions. In this study, controlled experiments and field observations were conducted to calibrate the fundamental relationships in various rainy conditions with various bidirectional pedestrian flow ratios at signalized crosswalks in Hong Kong. A potential field cellular automaton simulation model was proposed to investigate walking behavior at crosswalks in rainy conditions, such as pedestrians' lifting or lowering their umbrellas, which resulted in the umbrellas overlapping during the crossing process. The simulation results show that the proposed model can reproduce the phenomenon of quick-forming pedestrian streams for pedestrians with umbrellas at signalized crosswalks. Rainfall intensity and the pedestrian bidirectional flow ratio have various effects on average walking speeds. The proposed simulation model is particularly useful for the design of intersections with signalized crosswalks in Asian cities with relatively high annual rainfall intensity.

Keywords: Walking behavior, Signalized crosswalk, Rainfall intensity, Bidirectional flow ratio

1. INTRODUCTION

Crosswalks are essential facilities for pedestrians and drivers. Pedestrian walking characteristics at crosswalks are useful for the design of intersections, to which much attention has been paid by researchers from multiple disciplines, such as physics, mathematics, engineering, and sociology (Transportation Research Board, 2000; Lam and Cheung, 2000; Lam *et al*., 2002; Zeng *et al*., 2014).

Generally, two methods, including statistical and simulation-based methods, are used for such studies. For statistical methods, field data are collected and analyzed to investigate the effects of certain key factors on walking characteristics at crosswalks. Such factors include age, gender, group behavior, weather, and pedestrian compliance. Lam and Cheung (2000) and Lam *et al*. (2002) collected field data to investigate the bidirectional effects and found that the effective capacity and average walking speed at capacity depended on the bidirectional flow ratio. Simulation is another frequently used method. Various models have been proposed to simulate walking behavior at crosswalks, ranging from the social force model (Zeng *et al*., 2014) and the floor field model (Li and Dong, 2012; Lu *et al*., 2014), to the agent-based model (Liu *et al*., 2014). In addition, Lee and Lam (2008) presented the calibration of a simulation model for pedestrian movement at signalized crosswalks in Hong Kong, in which the effects of bidirectional pedestrian flow (i.e., the effect of the flow ratio) on the average walking speed and the level of service for crosswalks were emphasized.

Furthermore, some researchers (e.g. Prevedouros and Chang, 2005; Lam *et al*., 2008) have investigated the effects of rainfall on traffic flow particularly for tropical and subtropical cities, such as Hong Kong which has the average annual rainy days with 141.6 days in the past ten years (2007-2016, where the average annual rainfall intensity is over 2,300 mm, http://www.hko.gov.hk). However, these works have focused on vehicular flow instead of pedestrian flow. As shown in Figure 1, walking behavior at signalized crosswalks in rainy conditions can differ considerably from that in normal conditions. Chang *et al*. (2011) conducted a field survey with video cameras and found that the mean walking speed under conditions of no rain (1.22 m/s) was significantly higher than that in rainy conditions (0.85 m/s). Nevertheless, models of pedestrian movements at signalized crosswalks in adverse weather conditions remain limited.

(a) In normal condition without rain (b) In rainy condition

Figure 1. Comparison of pedestrian movements in normal and rainy conditions at a signalized crosswalk in Hong Kong

To fill this gap, this study aims to calibrate the fundamental speed-density relationships to account for bidirectional flow effects in rainy conditions and to propose a simulation model to capture pedestrian walking behavior in various rainy conditions at signalized crosswalks in Hong Kong.

The remainder of this paper is organized as follows. Section 2 studies the calibration of walking speeds for bidirectional flow in rainy conditions. A potential field cellular automaton simulation model is presented in Section 3, in which walking strategies and basic updating rules are discussed. The simulation results and analyses for the effects of rainfall intensity and the bidirectional flow ratio on the average walking speed are presented in Section 4. Finally, conclusions and directions for future study are given in Section 5.

2. CALIBRATION OF PEDESTRIAN SPEED-DENSITY RELATIONSHIP IN RAINY CONDITIONS

In rainy conditions, pedestrians hold umbrellas while crossing intersections. In practical terms, the maximum pedestrian density and fundamental speed-density relationship differ considerably from those in normal conditions without rain. When a pedestrian with an umbrella is unable to walk freely, especially when facing heavy opposing pedestrian flow, he or she may lift or lower the umbrella or even slant it to walk through the crosswalk as quickly as possible. In this case, some umbrellas begin to overlap (dashed rectangles shown in Figure 2) during the crossing process. To investigate such walking characteristics at signalized crosswalks in rainy conditions, controlled experiments were conducted at an outdoor site. A potential field cellular automaton simulation model was then proposed to capture the walking behavior in rainy conditions.

2.1 Controlled Experiments

Controlled experiments were conducted in the Road Research Laboratory of the Hong Kong Polytechnic University on May 26, May 27, and June 11, 2016. The Laboratory is located on an off-street that provides an outdoor environment for experiments. More than 120 participants were recruited for these three controlled experiments. A sprinkler system was installed at the experimental site to imitate real rainy conditions. The testing scenarios were designed based on several controlled variables, such as rainfall intensity, the number of pedestrians, and the bidirectional pedestrian flow ratio. Five video cameras were set to capture the pedestrians' movements. A snapshot of one of the controlled experiments is shown in Figure 2, and the measurement area is described in Figure 3.

Figure 2. Snapshot of pedestrian controlled experiment

2.2 Data Extraction

Data extraction was carried out with a semi-automated video technique. A computer program was made to record from videotape the times at which pedestrians crossed a measurement section (Lam and Cheung, 1998).

As shown in Figure 3, a pedestrian was selected, and his or her entry and exit times while crossing the measurement section were recorded. Two pedestrian streams *a* and *b* moved in opposite directions at the designed crosswalk. Specifically, the times at which a pedestrian from stream *a* passed Lines 2 and 3 were recorded as t_1 and t_2, respectively. The walking speed v_a (m/min) during this time interval was obtained by $(t_2\text{-}t_1)/d$, where d is the distance between Lines 2 and 3. Moreover, the time at which each pedestrian crossed the central line of the measurement section was recorded and stored. We counted the pedestrians of streams *a* and *b*, respectively, as they passed the Central line (I) and thus obtained flow profiles *a* and *b*. The one-way pedestrian flow rates f_a and f_b (person/min/m) during $t_2\text{-}t_1$ were then taken as the average number of pedestrians who passed the central line in unit time and unit width for streams *a* and *b*, respectively. The pedestrian bidirectional flow ratio r_a was taken as $f_a/(f_a+f_b)$. As such, the walking speed v_a corresponded to one-way pedestrian flow f_a and flow ratio r_a.

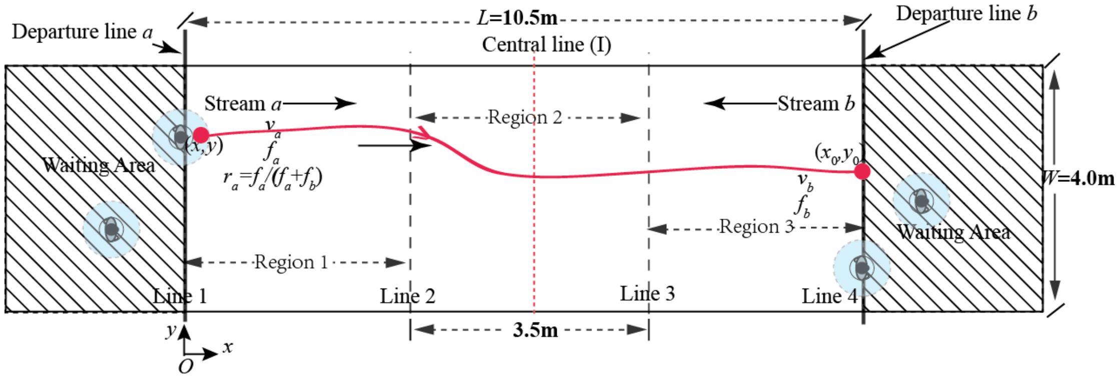

Figure 3. Illustration of the designed crosswalk and measurement section for the controlled experiments

2.3 Fundamental Relationship for Bidirectional Pedestrian Flow in Rainy Conditions

We study the relationship between walking speed v_a and one-way pedestrian flow f_a, or walking speed v_a and pedestrian density ρ_a (i.e., f_a/v_a) under various pedestrian bidirectional flow ratios r_a and rainfall intensities *I*, denoted as $v_a = F(\rho_a, r_a, I)$. The following function is proposed to estimate the above relationship based on the extracted data (Lam *et al*., 2013):

$$v_a(\rho_a, r_a, I) = V_f(I)\exp\left[(-4.10 + 5.22r_a - 2.49r_a^2)\left(\frac{\rho_a}{1+2.69r_a}\right)\right], \tag{1}$$

where $V_f(I)$ is the free-flow walking speed of pedestrians with umbrellas at a rainfall intensity *I*. The observed average free-flow walking speed decreased from 73.60 m/min to 55.50 m/min with the rainfall intensity increased from 0.10 mm/h to 15.00 mm/h, and it was calibrated as $V_f(I) = \exp\left(4.1817I^{-0.0147}\right)$.

The comparison between the observed and estimated data in light rain conditions is shown in Figure 4, where the rainfall intensity is about 0.10 mm/h. The R^2 value of 0.83 gives promising fitting results for use of the calibration function (1) in the simulation model proposed below.

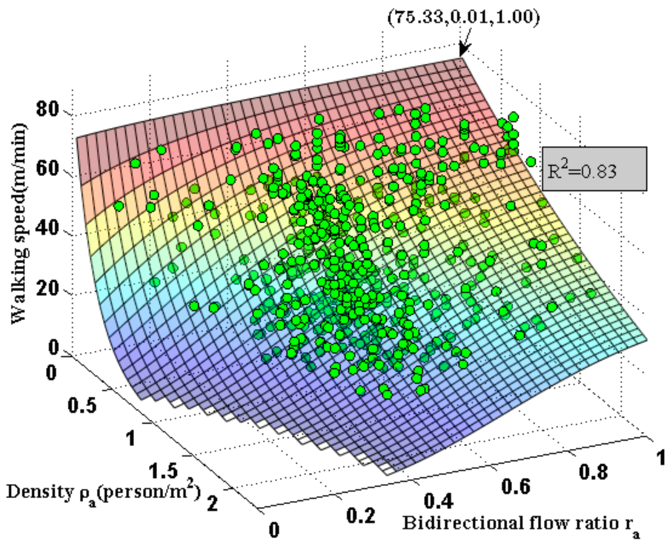

(75.33, 0.01, 1.00) represents walking speed = 75.33 m/min, density of pedestrian stream *a* ρ_a= 0.01 person/m^2, and flow ratio r_a = 1.00

Figure 4. Walking speed against pedestrian density and bidirectional flow ratio

3. SIMULATION MODEL

3.1 Assumptions

The following assumptions are made to facilitate the presentation of the essential ideas in this paper.

A1. In rainy conditions, all pedestrians hold umbrellas when crossing a signalized crosswalk. Although some pedestrians use raincoats and some do not carry umbrellas in light rain conditions, it is straightforward to extend the results from the proposed model.

A2. In general, the diameter of an umbrella is 0.95 to 1.05 m. In this study, we assume that all umbrellas have a diameter of 1.00 m.

A3. The personal characteristics of pedestrians are assumed to be homogeneous. In other words, characteristics such as gender and age are not considered.

3.2 Occupied Cells of a Pedestrian with an Umbrella

The multi-grid method (Bandini *et al.*, 2014), which is a widely used approach to localizing pedestrians in a 2D simulation, is adopted to capture the overlapped umbrella effect. The studied crosswalk is discretized into small cells of 0.20×0.20 m^2. Each umbrella occupies 25 cells (Figure 5). The 25 occupied cells are denoted by (i, j), i, j = -2, -1, 0, 1, 2, with its central cell at (0, 0). We use a Moore neighborhood (Packard and Wolfram, 1985) in this study, that is, an umbrella can be moved in one of eight directions or remain still (Figure 5(b)). If the umbrella is moved one cell, its twenty-five occupied cells move together. In this case, for simplicity, we use the movement of the umbrella's central cell to represent its entire movement.

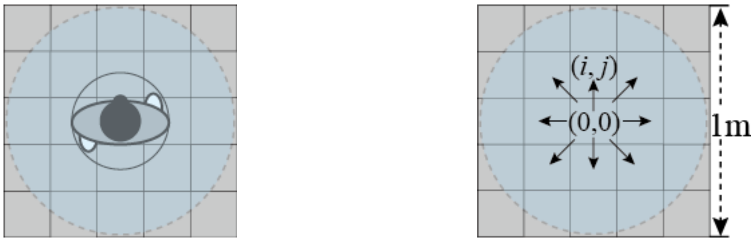

(a) Single pedestrian with an umbrella (b) Moore neighborhood

Figure 5. Occupied cells of umbrella

3.3 Walking Strategy based on a Cost Potential Field

To derive the optimal walking direction, a cost potential field is proposed based on Jian *et al*. (2014) in the following.

As shown in Figure 3, at position (x, y) and at time t, we consider the movement of a pedestrian with free-flow walking speed $V_f(I)$ at a rainfall intensity I. The cost distribution of such a pedestrian is his or her time of walking unit distance and is denoted by $C(\rho(x,y),t,I)$, i.e., $C(\rho(x,y),t,I)=1/V(x,y,t,I)$, where $V(x,y,t,I)=V(V_f(I),\rho(x,y,t,I))$ is his or her walking speed and $\rho(x,y,t,I)$ is the local density.

However, two pedestrian streams a and b have opposite directions at the crosswalk. Stream c ($c=a$, b) would face the interactions with the opposing flow d ($d=b$, a). In view of the rain factor, the cost distribution of stream c can be extended from Zhang *et al*. (2012):

$$\tau_c(x,y,t,I)=C(\rho(x,y),t,I)\Gamma_c(\psi(x,y,t),\rho_c(x,y,t,I),\rho_d(x,y,t,I)),\ \ c=a,b;\ d=b,a \qquad (4)$$

where,

$\psi(x,y,t)$: the crossing angle of pedestrian streams a and b at (x,y),

$\rho=\rho_a+\rho_b$: the total density, and

$\Gamma_c(\psi,\rho_c,\rho_d)$: the scaling function to describe the avoiding and following features of pedestrian stream c.

Based on field studies (Wong *et al*., 2010; Xie *et al*., 2013) and numerical experiments (Zhang *et al*., 2012), we explicitly incorporate the bidirectional flow ratio into the scaling functions:

$$\Gamma_c(\psi,\rho_c,\rho_d)=$$
$$\exp\left(\beta_1(r_c)(1-\cos\psi(x,y,t))\rho_d(x,y,t)\right)\cdot\exp\left(-\beta_2(r_c)w_c(x,y)\rho_c(x,y,t)\right), c=a,b \qquad (5)$$

where r_c is the flow ratio for pedestrian stream c, that is, r_c = flow of stream c/two-way flow.

The first exponential term of Equation (5) is denoted by EXP_c^1, and it should satisfy the property of monotonicity, that is, $\partial\mathrm{EXP}_c^1/\partial\rho_d\geq 0$, which indicates the avoiding nature of pedestrians. Regarding the second exponential term EXP_c^2 of Equation (5), we have $\partial\mathrm{EXP}_c^2/\partial\rho_c\leq 0$, which reflects the following nature of pedestrians.

At time t, we consider the minimal generalized cost of the pedestrian in stream c from position (x, y) to destination D_c (c = a or b). Based on the cost distribution $\tau_c(x,y,t,I)$, there uniquely exists a function $\varphi_c(x,y,t,I)$, that is, the cost potential field, that satisfies the following Eikonal equations (Zhang *et al*., 2012; Jian *et al*., 2014):

$$\sqrt{\left(\frac{\partial \varphi_c}{\partial x}\right)^2 + \left(\frac{\partial \varphi_c}{\partial y}\right)^2} = \tau_c(x, y, t, I), \quad \varphi_c(x_0, y_0, t, I) = 0, \quad c = a, b \tag{6}$$

where $(x_0, y_0) \in D_c$.

In fact, $\varphi_c(x, y, t, I)$ is the minimum cost from origin $A(x,y)$ to destination $B(x_0, y_0) \in D_c$. Therefore, walking along the negative gradient direction of the cost potential field would be the optimal path choice, which is also called a reactive user optimal walking strategy. Such a direction is the steepest descent of the cost potential field. Thus, we have the crossing angle in Equation (5) that

$$\psi(x, y, t, I) = < -\nabla\varphi_a(x, y, t, I), -\nabla\varphi_b(x, y, t, I) >. \tag{7}$$

We adopt the fast sweeping method (Zhao, 2005) to solve the coupled Equations (6) and (7). Actually, the right-hand side of Equation (6) contains Equation (7). The potential fields at discrete time t_{i-1}, that is, $\varphi_c(x, y, t_{i-1}, I), c = a, b$, are used to approximate those at time t_i in the computation of the crossing angle in Equation (7) (Zhang *et al*., 2012).

Based on the calibrated fundamental relationship in Section 2.3, the walking speed for bidirectional pedestrian flow in rainy conditions in the simulation model is obtained. In contrast, the flow ratio in Equation (5) for the cost distribution can also be determined. Specifically, we first reconstruct the pedestrian densities ρ_a and ρ_b (see Appendix) and then obtain $v_a = F(\rho_a, r_a, I)$ and $v_b = F(\rho_b, r_b, I)$ from Equation (1). Notice that $r_a = \rho_a v_a / (\rho_a v_a + \rho_b v_b)$. We thus get flow ratio r_a by solving the coupled equations.

3.4 Basic Updating Rules

To further facilitate the discussion, a variable $O(i, j)$ is introduced to represent the number of umbrellas occupying cell (i, j); that is, $O(i, j) = k$ means that the cell is occupied by k umbrella(s), and it is dynamically updated in the whole simulation. If the cell is newly occupied or newly vacated by an umbrella, the value is updated as $O(i, j) = O(i, j)+1$ or $O(i, j) = O(i, j)-1$, respectively.

3.4.1 Feasible walking schemes

Pedestrians holding umbrellas do their best to minimize conflict delays with opposing pedestrians. If there is not enough empty space to move forward, a pedestrian holding an umbrella may try to lift or lower his or her umbrella to minimize the conflict. Based on this assumption, we discuss the following two stages by combining the potential field to determine whether a pedestrian lifts or lowers his or her umbrella.

(1) Stage I: Walking without lifting or lowering umbrella

When a pedestrian moves one cell in a perpendicular or diagonal direction as shown in Figure 6, some newly occupied cells will emerge. Such newly occupied cells are described as follows:

1) Walking in a perpendicular direction, i.e., $i = 0, j = \pm 1$ or, $i = \pm 1$, $j = 0$ (Figure 6(a)):

$$\Omega_{\mathrm{NOC}}^{1}(i,j)=\left\{\left(k(1-i^2)+3i,\, k(1-j^2)+3j\right) \mid k=-2,-1,0,1,2\right\}, \tag{8}$$

2) Walking in a diagonal direction, i.e., $i=\pm 1, j=\pm 1$ (Figure 6(b)):

$$\Omega_{\mathrm{NOC}}^{2}(i,j)=\left\{\left(3i,\, j+k\right) \mid k=-2,-1,0,1,2\right\}\cup\left\{\left(i+k,\, 3j\right) \mid k=-2,-1,0,1,2\right\}. \tag{9}$$

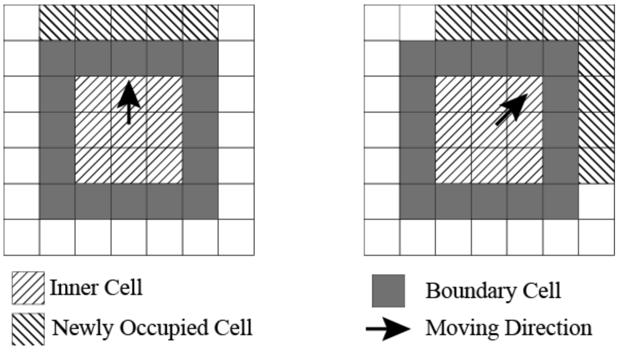

(a) Perpendicular walking direction (b) Diagonal walking direction

Figure 6. Case of walking without lifting or lowering umbrella

If the newly occupied cells are empty or available for a person to enter, there is no need to lift or lower his or her umbrella. Thus, the movement of the person at the central cell from (0, 0) to (i, j) in this case is defined as feasible if it satisfies two conditions: (1) the newly occupied cells are empty and (2) the potential value of the central cell is declined. Specifically,

if $i=0, j=\pm 1$ or $i=\pm 1, j=0$, then

$$\sum_{(\tilde{i},j)\in\Omega_{\mathrm{NOC}}^{1}(i,j)} O(\tilde{i},j)=0 \ \text{ and } \ \varphi(i,j)\le\varphi(0,0)\text{; or} \tag{10a}$$

if $i=\pm 1, j=\pm 1$, then

$$\sum_{(\tilde{i},j)\in\Omega_{\mathrm{NOC}}^{2}(i,j)} O(\tilde{i},j)=0 \ \text{ and } \ \varphi(i,j)\le\varphi(0,0). \tag{10b}$$

The set of the new central cell (i, j) of all of the feasible walking schemes at Stage I is denoted by $\Omega_{\mathrm{Feasi}}^{1}$.

(2) Stage II: Walking with lifting or lowering umbrella

If $\Omega_{\mathrm{Feasi}}^{1}=\varnothing$, the pedestrian will adjust the level of the umbrella by lifting or lowering it to walk, and umbrellas then begin to overlap. In view of this, some cells are jointly occupied by such umbrellas (Figure 7). The new inner cells depicted in Figure 7 are introduced at the second stage. Similarly, the new inner cells can be described as follows.

1) Walking in a perpendicular direction, i.e., $i=0, j=\pm 1$ or, $i=\pm 1$, $j=0$ (Figure 7(a)):

$$\Omega_{\mathrm{NIC}}^{1}(i,j)=\left\{\left(k(1-i^2)+2i,\, k(1-j^2)+2j\right) \mid k=-1,0,1\right\}. \tag{11}$$

2) Walking in a diagonal direction, i.e., $i=\pm 1, j=\pm 1$ (Figure 7(b)):

$$\Omega^2_{\mathrm{NIC}}(i,j)=\{(2i,\ j+k)\,|\,k=-1,0,1\}\cup\{(i+k,\ 2j)\,|\,k=-1,0,1\}. \tag{12}$$

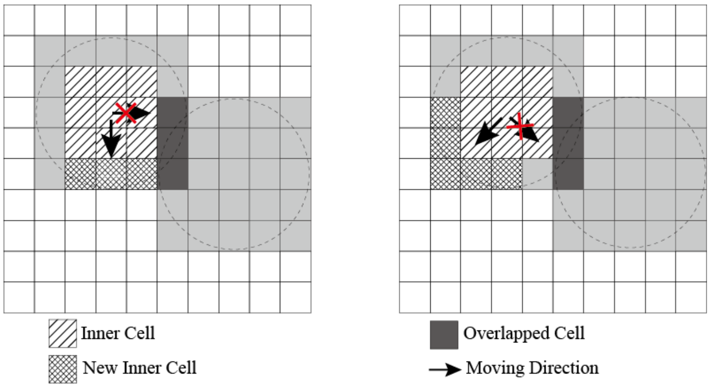

(a) Perpendicular walking direction (b) Diagonal walking direction

Figure 7. Case of walking with lifting or lowering umbrella

As shown in Figure 7, a cross "×" represents that the walking direction is not allowed because the new inner cells have been occupied by other umbrella(s). To avoid being overcrowded, this strategy also indicates that the jointly occupied cells can occur only on the boundary cells.

In this case, feasible walking should satisfy two conditions: (1) the new inner cells are occupied by the umbrella itself and (2) the potential value of the central cell is declined. Similarly, it should satisfy the following equations:

if $i=0, j=\pm1$ or $i=\pm1, j=0$, then

$$\prod_{(\tilde{i},j)\in\Omega^1_{\mathrm{NIC}}(i,j)} O(\tilde{i},j)=1 \ \text{ and } \ \varphi(i,j)\le\varphi(0,0)\text{; or} \tag{13a}$$

if $i=\pm1, j=\pm1$, then

$$\prod_{(\tilde{i},j)\in\Omega^2_{\mathrm{NIC}}(i,j)} O(\tilde{i},j)=1 \ \text{ and } \ \varphi(i,j)\le\varphi(0,0). \tag{13b}$$

The set of the new central cell (i, j) of all of the feasible walking schemes at Stage II is denoted by $\Omega^2_{\mathrm{Feasi}}$.

3.4.2 Optimal walking schemes

To choose an optimal walking scheme from all of the alternatives, it is expected that the pedestrian walks toward the steepest descent of the potential field. Nevertheless, a pedestrian occupies 25 cells, and they all move together with the movement of the pedestrian. Let $\bar{\varphi}(i,j)$ be the decline of the average cost divided by 25 cells, i.e.,

$$\bar{\varphi}(i,j)=\frac{1}{25}\frac{\sum_{(p,q)\in\Omega_{\mathrm{Index}}}\varphi(0+p,0+q)-\varphi(i+p,j+q)}{\sqrt{i^2+j^2}\mathrm{d}l},\quad (i,j=0,\pm1), \tag{14}$$

where $\Omega_{\mathrm{Index}}=\{(p,q)\,|\,p,q=0,\pm1,\pm2\}$ is the index set of the occupied cells and dl = 0.20 m is the length of a cell's side.

Therefore, the expected walking strategy is that the pedestrian will choose the one with the steepest descent over $\bar{\varphi}(i, j)$ instead of $\varphi(i, j)$ from all feasible walking schemes. Specifically,

(1) If $\Omega^1_{\text{Feasi}} \neq \varnothing$, denote $\Omega_{\text{Opti}} = \left\{(i^*, j^*) \mid \bar{\varphi}(i^*, j^*) \geq \bar{\varphi}(i, j),\ \ (i, j) \in \Omega^1_{\text{Feasi}}\right\}$,

(2) If $\Omega^1_{\text{Feasi}} = \varnothing$, $\Omega^2_{\text{Feasi}} \neq \varnothing$, denote $\Omega_{\text{Opti}} = \left\{(i^*, j^*) \mid \bar{\varphi}(i^*, j^*) \geq \bar{\varphi}(i, j),\ \ (i, j) \in \Omega^2_{\text{Feasi}}\right\}$.

If $\left|\Omega_{\text{Opti}}\right| = 1$, then the pedestrian will choose the only element of Ω_{Opti} to move toward.

If $\left|\Omega_{\text{Opti}}\right| > 1$, move to each cell in Ω_{Opti} with the probability $1/\left|\Omega_{\text{Opti}}\right|$.

If $\Omega^1_{\text{Feasi}} = \varnothing$, $\Omega^2_{\text{Feasi}} = \varnothing$, keep still.

3.5 Walking Speed Variation in Cellular Automaton Model

As pedestrians dynamically alter their walking speeds during the walking process, it is essential to study the walking speed variation in a cellular automaton model. To reflect realistic walking behavior, each updating time step is sufficient for walking one step for the quickest pedestrian. We denote the maximum free-flow walking speed of all pedestrians by $V_{f,\max}(I)$ and the width of each cell as Δl m (e.g. $\Delta l = 0.20$ in our proposed model). We take $\Delta t = n\Delta l / V_{f,\max}(I)$ such that $n\Delta l$ is approximately equal to one step length. In fact, such a time step is also beneficial for the computation of potential field, especially for the multi-grid method. The fastest pedestrians can then walk at most n cells at each time step.

To consider the movement of a pedestrian with a desired walking speed of $V(I)$ ($V(I) \leq V_{f,\max}(I)$) in each updating time step, we extend the method proposed by Yuan and Tan (2007). During time step t_i, a probability $p_i = V(I)/V_{f,\max}(I)$ is introduced to describe his or her walking behavior. Each updating time step can be divided into n sub-steps, denoted by $t_i^{(k)}$, k=1, 2, …, n. At sub-step $t_i^{(k)}$, the pedestrian has two choices: (1) to walk with a probability p_i and (2) to keep still with a probability 1-p_i.

3.6 Simulation Procedure

From the above discussion, the main procedures of the simulation are summarized as follows.

(I) At updating time step t_i: Potential fields are obtained by solving Eikonal equations (6) and (7) using the Fast Sweeping method. All pedestrians are updated in a random serial order. For a specific individual at sub-step $t_i^{(k)}$, k=1, 2, …, n:

(i) Determine the optimal walking scheme based on the updating rules defined in Section 3.4.

(ii) Walk toward the optimal walking scheme with a probability or keep still with the other corresponding probability in Section 3.5.

(II) Increment $t_{i+1} = t_i + \Delta t$, repeat (I) until the end of the green time of that particular walking phase.

4. SIMULATION EXPERIMENT

In the simulation experiment, the width and length of the signalized crosswalk are adopted as W = 12.60 *m* and L = 18.20 m, the sum of the pedestrian green and flashing green times is set as 43 s, and the pedestrian red time is set as 77 s. Other parameters are taken as follows: the generalized cost distribution $C(\rho) = \exp(0.3\rho^2)/V_f(I)$ in Equation (4) and $\beta_1(r_c) = 0.21(1-r_c)$, $\beta_2(r_c) = 0.11r_c$ in Equation (5).

4.1 Lane Formation

Figure 8 presents the simulation snapshots of the lane formation at balanced pedestrian flows (i.e., the pedestrian flows on both sides of the crosswalk are equal). In this simulation, the rainfall intensity is taken as 1.00 mm/h. We can easily observe that the phenomenon of lane formation is reproduced in the proposed model with the consideration of pedestrians' lifting or lowering their umbrellas. It should be also noted that this model is able to quickly form streams at the signalized crosswalk, which is a challenge and therein a contribution of the proposed model compared with the simulation at other scenarios such as sidewalks.

Figure 8. Simulation snapshots of lane formation

4.2 Effects of Rainfall Intensity and Bidirectional Flows on Walking Speed

To further obtain walking characteristics such as the average walking speed, the times at which each pedestrian passed the two departure lines and the central line of the crosswalk (as shown in Figures 3 and 8) were all recorded in the simulation. The number of pedestrians who passed the central line of the measurement section in unit time and unit width for each pedestrian stream was counted as the flow rate.

We first focus on the effects of rainfall intensity and bidirectional pedestrian flows on the average walking speed. In the simulation, the bidirectional pedestrian flows at the crosswalk are balanced and the signal cycles are repeated 35 times.

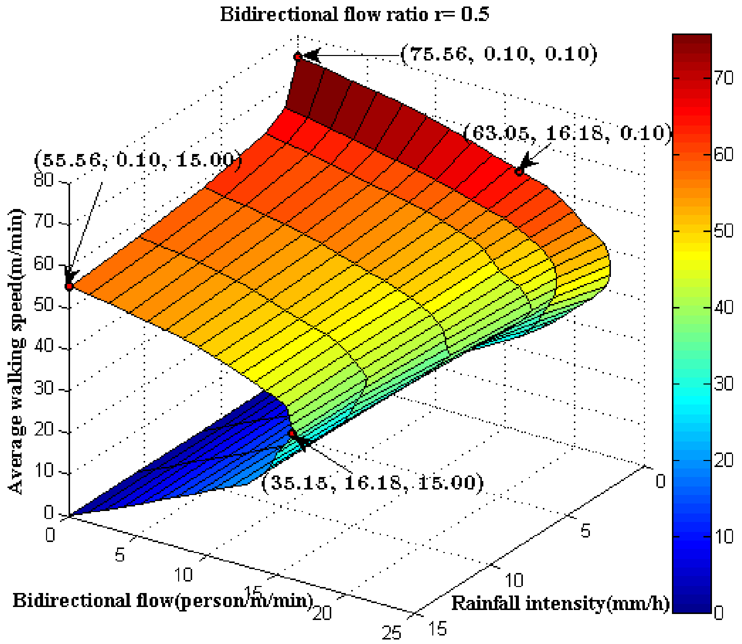

(35.15, 16.18, 15.00) represents average walking speed = 35.15 m/min, bidirectional pedestrian flow = 16.18 person/m/min, rainfall intensity = 15.00 mm/h

Figure 9. Average walking speed against bidirectional pedestrian flow and rainfall intensity

Figure 9 shows the average walking speed against rainfall intensity and bidirectional pedestrian flow. The maximum average walking speed of 75.56 m/min occurs at a low flow and in light rain condition; that is, the bidirectional pedestrian flow is 0.10 person/m/min and the rainfall intensity is 0.10 mm/h. It also shows the average walking speed deceases with the increase in rainfall intensity. At a low flow condition, i.e., the bidirectional pedestrian flow is 0.10 person/m/min, the average walking speed decreases from 75.56 to 55.56 m/min with an increase in the rainfall intensity from 0.10 to 15.00 mm/h. This is consistent with the calibrated result of the free walking speed in rainy condition in Section 2.3.

With a rainfall intensity of 15.00 mm/h, the average walking speed decreases from 55.56 to 35.15 m/min with an increase in the bidirectional pedestrian flow from 0.10 to 16.18 person/m/min, i.e., from the free-flow condition to a saturated flow condition. The rate of decrease reaches 58.07%. For the case of bidirectional pedestrian flow of 16.18 person/m/min, the average walking speed reaches 63.05 m/min with a rainfall intensity of 0.10 mm/h. The results indicate that the effects of rainfall intensity and bidirectional pedestrian flow on walking speed are significant.

4.3 Walking Speed Distributions

We investigate the walking speed distributions with balanced pedestrian flows in this section. Figure 10 shows the frequency distribution and the cumulative frequency distribution of walking speeds in the cases of light rain (1.00 mm/h) and heavy rain (15.00 mm/h) at a low bidirectional pedestrian flow (6.00 person/m/min). As shown in Figure 10, the walking speeds in both cases follow Gaussian distributions. We find that the walking speeds in light rain conditions are faster than those in heavy rain, which is consistent with the calibrated result in Section 2.3. The results also demonstrate that the walking speed variation proposed in Section 3.5 is valid in the simulation model.

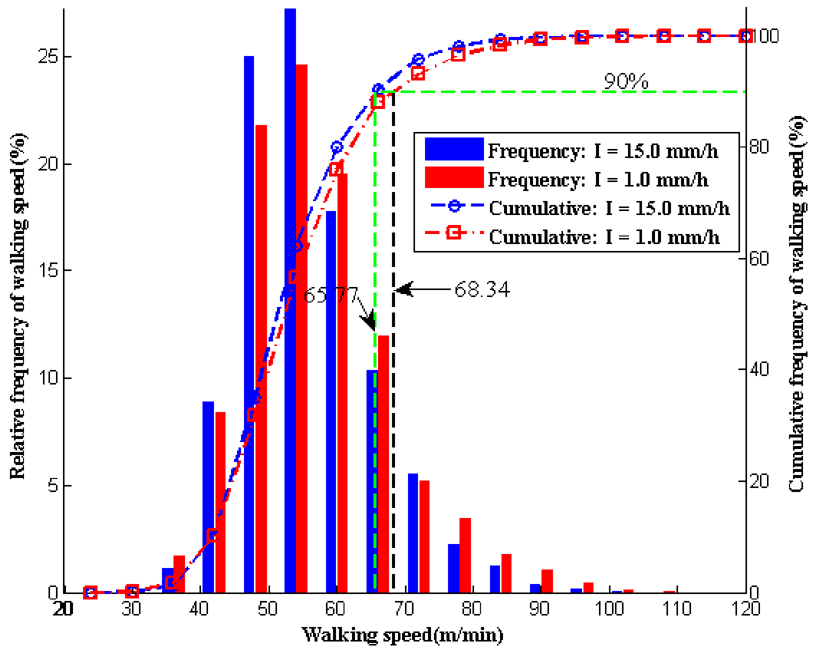

Figure 10. Frequency distribution and cumulative frequency distribution of walking speeds

4.4 Effects of Bidirectional Flow Ratio on Walking Speed

We next study the impacts of pedestrian bidirectional flow ratio at signalized crosswalks on the walking speed.

Table 1 shows the average walking speed against the bidirectional flow ratio in light and heavy rain conditions. As shown in Table 1, the average walking speed increases as the bidirectional flow ratio increases with the same rainfall intensity and the same bidirectional flow condition. At a less congested two-way pedestrian flow of 10.00 person/m/min and a rainfall intensity of 1.00 mm/h, specifically, the average walking speed increases from 50.09 to 60.78 m/min with an increase in the bidirectional flow ratio from 0.25 to 1.00. The rate of increase reaches 21.34%. At a congested two-way pedestrian flow of 16.00 person/m/min and a rainfall intensity of 1.00 mm/h, however, the rate of increase reaches 248.32% from 16.64 to 57.96 m/min. This demonstrates that the effects of the bidirectional flow ratio on the walking speed are significant, which is consistent with the results of the Highway Capacity Manual (Transportation Research Board, 2000) and Lee and Lam (2008).

Table 1. Impacts of bidirectional flow ratio on average walking speed (m/min) under light and heavy rain conditions

Two-way pedestrian flow, Rainfall intensity \ Bidirectional flow ratio		0.25	0.50	0.75	1.00
Less congested, 10.00 person/m/min	1.00 mm/h	50.09	51.72	54.15	60.78
	15.00 mm/h	42.06	43.13	45.85	50.96
Congested, 16.00 person/m/min	1.00 mm/h	16.64	41.93	45.73	57.96
	15.00 mm/h	14.74	33.45	37.79	47.97

4.4 Comparison between the scenarios of pedestrians with and without umbrellas

We finally focus on the comparison between the scenarios of each pedestrian with an umbrella and pedestrians without umbrellas. In fact, the maximum bidirectional pedestrian flows and the jam densities for both scenarios differ considerably. Figure 11 shows the walking speed against the bidirectional pedestrian flow for both cases in light and heavy rain conditions, where the bidirectional flow ratio is 0.5. In light rain condition with a rainfall intensity of 1.00 mm/h, as shown in Figure 11(a), the maximum bidirectional pedestrian flow for case of each pedestrian with an umbrella is 19.64 person/m/min, which is almost half that of the latter case, i.e., 40.18 person/m/min. The critical walking speeds of both cases are 38.16 and 23.67 m/min, respectively. When the rainfall intensity increases from 1.00 to 15.00 mm/h, the maximum bidirectional pedestrian flow decreases from 19.64 to 16.68 person/m/min in the scenario of each pedestrian with an umbrella, together with the critical walking speeds decreases from 38.16 to 32.41 m/min.

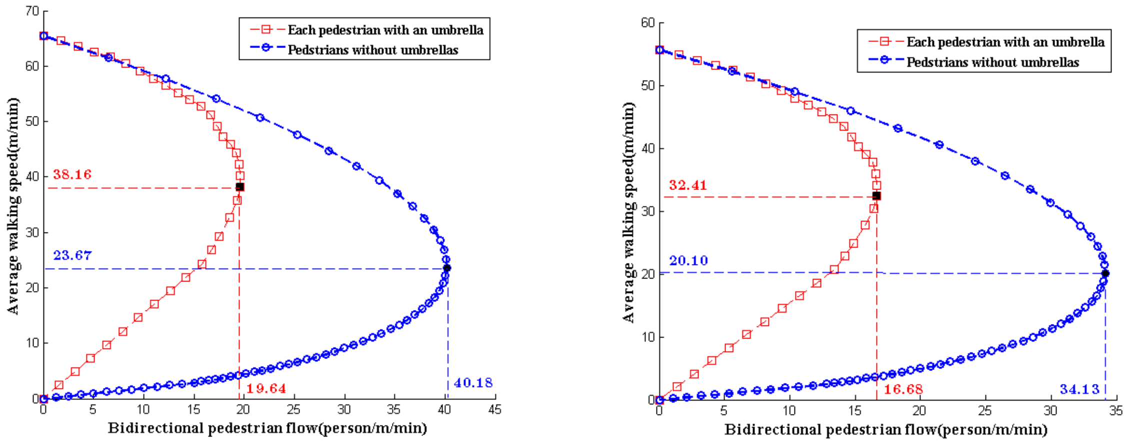

(a) Light rain, I = 1.00 mm/h (b) Heavy rain, I = 15.00 mm/h

Figure 11. Comparison of average walking speed against bidirectional flow between the scenarios of pedestrians with and without umbrellas (bidirectional flow ratio r = 0.5)

From the above discussion, we can conclude that factors such as the rainfall intensity, the bidirectional pedestrian flow, and the bidirectional flow ratio have various effects on the walking speed. Such results demonstrate that the proposed model can practically simulate the walking behavior of pedestrians in rainy conditions.

5. CONCLUSIONS

In this paper, a calibrated and robust simulation model is proposed to investigate walking behavior at signalized crosswalks in rainy conditions. When walking across crosswalks on rainy days, pedestrians lift or lower their umbrellas, and the umbrellas may overlap. To capture these walking behaviors, we carried out controlled experiments and field observations to calibrate the fundamental relationship for bidirectional flow and free-flow walking speeds in rainy conditions.

The simulation results indicate that the proposed model succeeds in reproducing the phenomenon of quick-forming streams at congested signalized crosswalks with consideration of pedestrians' lifting or lowering their umbrellas, particularly when the pedestrian bidirectional flow is imbalanced. The proposed model can simultaneously consider the following and avoiding features for pedestrians at signalized crosswalks in rainy conditions. The simulation results show that many factors, such as the rainfall intensity, bidirectional pedestrian flow, and flow ratio, have various effects on walking speeds.

The proposed simulation model is particularly useful for designing intersections with signalized crosswalks in many Asian cities with relatively high annual rainfall intensity and heavy pedestrian flows. The multi-grid method presented in this paper also contributes to modeling pedestrian walking behavior in overcrowded conditions by considering the degree of overlap for the occupied areas of their bodies. The proposed approach can be extended to investigate the effects of different groups of pedestrians (e.g., by gender and age group) to design walking facilities in densely populated urban areas for rainy conditions. In particular, some pedestrians may use raincoats, and some may not use umbrellas when it is not raining heavily.

In this paper, the size of the crosswalk, the traffic signal time, and the size of the umbrellas are fixed in the simulation experiment. Further research is required to consider different sizes of crosswalk and traffic controls (both signalized and non-signalized) and different sizes of umbrella to investigate empirically their effects on pedestrian walking behavior at crosswalks in various rainfall intensities.

ACKNOWLEDGEMENTS

The work was supported by grants from the Research Grants Council of the Hong Kong Special Administrative Region (Project No. PolyU 5243/13E), National Science Foundation of China (Project No. 11672348), and the National Basic Research Program of China (Project No. 2012 CB725404).

APPENDIX: RECONSTRUCTION OF PEDESTRIAN DENSITY

Each umbrella carried by an individual occupies 25 cells, and each cell contains 1/25 of a pedestrian.

1/25	1/25	1/25	1/25	1/25
1/25	1/25	1/25	1/25	1/25
1/25	1/25	1/25	1/25	1/25
1/25	1/25	1/25	1/25	1/25
1/25	1/25	1/25	1/25	1/25

Figure A1. Illustration of distribution of pedestrian(s)

The density of the cell located at position (x, y) can be reconstructed by taking the weighted average over the cells within a square $A(x, y)=\{(p, q)|p, q = -m, -m+1,\ldots,m\}$, which has $(2m+1)^2$ cells with its central cell at (x, y):

$$\rho(x,y)=\sum_{(p,q)\in A(x,y)}\frac{w(p,q)n_{\text{Ped}}(p,q)}{s},\quad \sum_{(p,q)\in A(x,y)} w(p,q)=1, \tag{A1}$$

where,

$n_{\text{Ped}}(p, q)$: the pedestrians in cell (p, q),

s : the area of each cell,

and the weighted function is

$$w(p,q)=\frac{\exp(-r^2(p,q)/R^2)}{\sum_{(\xi,\eta)\in A(x,y)}\exp(-r^2(\xi,\eta)/R^2)}, \tag{A2}$$

where $r(p, q)$ is the distance of cell (p, q) and (x, y), $R=\max_{(\xi,\eta)\in A(x,y)}\{r(\xi,\eta)\}$. We take m = 3 for the reconstruction of pedestrian density, that is, take the weighted average over 49 cells.

REFERENCES

Bandini, S., Mondini, M., Vizzari, G. (2014) Modelling negative interactions among pedestrians in high density situations. *Transportation Research Part C: Emerging Technologies*, 40, 251-270.

Chang, C.Y., Woo, T.H., Wang, S.F. (2011) Analysis of pedestrian walking speeds at crosswalks in Taiwan. *Proceedings of the Eastern Asia Society for Transportation Studies*, 8, 1186-2200.

Jian, X.X., Wong, S.C., Zhang, P., Choi, K., Li, H., Zhang, X. (2014) Perceived cost potential field cellular automata model with an aggregated force field for pedestrian dynamics. *Transportation Research Part C: Emerging Technologies*, 42, 200-210.

Lam, W.H.K., Cheung, C.Y. (1998) Pedestrian travel time functions for the Hong Kong underground stations – calibration and validation. *HKIE Transactions*, 5(3), 39-45.

Lam, W.H.K., Cheung, C.Y. (2000) Pedestrian speed/flow relationships for walking facilities in Hong Kong. *Journal of Transportation Engineering*, 126(4), 343-349.

Lam, W.H.K., Lee, J.Y.S., Cheung, C.Y. (2002) A study of the bidirectional pedestrian flow characteristics at Hong Kong signalized crosswalk facilities. *Transportation*, 29(2), 169-192.

Lam, W.H.K., Shao, H., Sumalee, A. (2008) Modeling impacts of adverse weather conditions on a road network with uncertainties in demand and supply. *Transportation Research Part B: Methodological*, 42(10), 890-910.

Lam, W.H.K., Tam M.L., Cao, X.Q., Li, X.M. (2013) Modeling the effects of rainfall intensity on traffic speed, flow, and density relationships for urban roads. *Journal of Transportation Engineering*, 139(7), 758-770.

Lee, J.Y.S., Lam, W.H.K. (2008) Simulating pedestrian movements at signalized crosswalks in Hong Kong. *Transportation Research Part A: Policy and Practice*, 42(10), 1314-1325.

Li, X., Dong, L.Y. (2012) Modeling and simulation of pedestrian counter flow on a crosswalk. *Chinese Physics Letters*, 29(9), 098902.

Liu, S.B., Lo, S.M., Ma, J., Wang, W.L. (2014) An agent-based microscopic pedestrian flow simulation model for pedestrian traffic problems. *IEEE Transactions on Intelligent Transportation Systems*, 15(3), 992-1001.

Lu, L.L., Ren, G., Wang, W., Wang, Y. (2014) Modeling walking behavior of pedestrian groups with floor field cellular automaton approach. *Chinese Physics B*, 23(8), 088901.

Packard, N.H., Wolfram, S., 1985. Two-dimensional cellular automata. *Journal of Statistical Physics*, 38(5), 901-946.

Prevedouros, P.D., Chang, K.W. (2005) Potential effects of wet conditions on signalized intersection LOS. *Journal of Transportation Engineering*, 131(12), 898-903.

Transportation Research Board (2000) *Highway Capacity Manual*. National Research Council, Washington, D.C.

Wong, S.C., Leung, W.L., Chan, S.H., Lam, W.H.K., Yung, N.H.C., Liu, C.Y., Zhang, P. (2010) Bidirectional pedestrian stream model with oblique intersecting angle. *Journal of Transportation Engineering*, 136(3), 234-242.

Xie, S.Q., Wong, S.C., Lam, W.H.K., Chen, A. (2013) Development of a bidirectional pedestrian stream model with an oblique intersecting angle. *Journal of Transportation Engineering*, 139(7), 678-685.

Yuan, W.F., Tan, K.H. (2007) A novel algorithm of simulating multi-velocity evacuation based on cellular automata modeling and tenability condition. *Physica A: Statistical Mechanics and its Applications*, 379(1), 250-262.

Zeng, W.L., Chen, P., Nakamura, H., Iryo-Asano M.H. (2014) Application of social force model to pedestrian behavior analysis at signalized crosswalk. *Transportation Research Part C: Emerging Technologies*, 40, 143-159.

Zhang, P., Jian, X.X., Wong, S.C., Choi, K. (2012) Potential field cellular automata model for pedestrian flow. *Physical Review E*, 85(2), 021119.

Zhao, H.K. (2005) A fast sweeping method for Eikonal equations. *Mathematics of Computation*, 74(250), 603-627.